eurofins | EAG Laboratories

APPLICATION NOTE

Understanding VCSELs: From Epitaxial Wafer Growth to Failure Analysis

By Charles Magee Ph.D., Michael Salmon Ph.D. and Temel Buyuklimanli Ph.D.

INTRODUCTION

The VCSEL has several advantages over its edge-emitting cousin. Its strengths include a higher modulation speed, on-wafer testing and the emission of a symmetrical emission pattern that is oriented perpendicular to the surface. This form of emission is ideal for coupling into other optical components. This emission pattern is also well suited for configuring multiple devices into a two-dimensional array,

However, all these merits over edge-emitting lasers come at the expense of a more complex device architecture. With a VCSEL, resonator mirrors have to fulfil two roles: like an edge-emitter, they have to control the extent of optical feedback and light output; but in addition, they also have to be electrically conducting, so that they can allow the injection of carriers from the contacts into the active region.

This set of requirements is often met by forming a stack of semiconductor layers, which have thicknesses that are carefully chosen to create a distributed Bragg reflector (DBR). To produce a high performance VCSEL, the DBR is formed from alternating layers with a sufficiently high refractive index contrast in order to realize high levels of reflection. Engineers must also ensure that the conductivity of the mirrors is sufficiently high to prevent current injection into the active region from causing excessive ohmic heating.

High-efficiency VCSELs are possible when these mirrors form part of a structure with a high degree of optical and electrical confinement. Such a device may be built from more than 200 layers, some of which can contain grading of both the doping level and the alloy composition. The typical resulting structure is shown in Figure 1.

Growth of such a structure is very challenging, so process engineers support their efforts by using a variety of characterization techniques to uncover details associated with the epilayers, such as their thickness, doping and composition. While some approaches can only offer insights into a few of these characteristics, one is capable of delivering a great deal of detail about these structure – is a variant of secondary ion mass spectrometry, known as **P**oint-by-point **COR**rected **SIMS**, or PCOR-SIMS. (For an overview of SIMS, please see: https://www.eag.com/techniques/mass-spec/secondary-ion-mass-spectrometry-sims/). Pioneered by our team at EAG Laboratories, this technique can measure layer thickness, composition and doping profile more accurately than regular

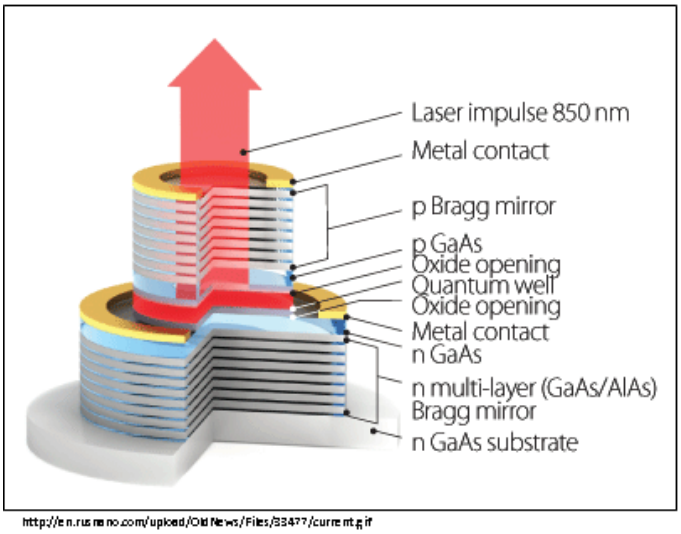

http://en.rusnano.com/upload/Old News/Files/33477/current.gif

Figure 1. Schematic drawing of an AlGaAs/GaAs VCSEL

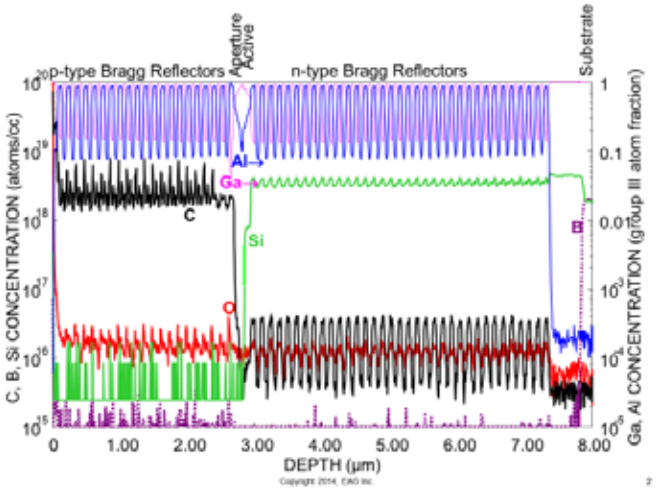

Figure 2. The PCOR-SIMS technique pioneered by EAG can provide a depth profile of a full VCSEL structure. All the profiles were acquired in a single analysis. The B profile marks the beginning of the substrate.

SIMS, where calibration with respect to alloy composition is not made for every data point (see Figure 2)

Our development of PCOR-SIMS can be traced back to the late 1990s when we were faced with acquiring accurate profiles for both dopants and matrix elements in SiGe materials. Prior to this

Understanding VCSELs: From Epitaxial Wafer Growth to Failure Analysis

time, it was commonly assumed that SIMS could not quantify matrix-level concentrations, and there was no way to change the dopant sensitivities continuously based on the matrix composition (because it was thought SIMS could not measure matrix composition). While PCOR-SIMS did not require any instrument modifications, many test samples had to be fabricated and analyzed by other techniques. These samples formed the basis for the empirical relationships between sensitivity and concentration that are the underpinnings of the PCOR-SIMS methodology. In addition, other techniques, both nuclear and TEM-based, were used to verify the accuracy of the final PCOR-SIMS results.

One of the biggest challenges associated with the application of SIMS to the analysis of AlGaAs/GaAs VCSELs is that variations in aluminum content impact the sensitivity of aluminum. This means that the quantitative analysis of aluminum content is not straightforward. Complicating matters further, changes in alloy composition affect the sensitivity of the dopant and impurity species measured in the depth profile.

PCOR-SIMS addresses these issues by employing empirically derived analytical functions to correct for the well-known 'SIMS matrix effect', which comes into play when one deals with materials that are dissimilar in nature. In addition, this advanced variant of SIMS can account for changes in dopant sensitivity which can be as much as a factor of two. The difference between traditional SIMS – where a single sensitivity is used in all layers – and PCOR-SIMS is illustrated in Figure 3. This shows the results of attempts to measure the silicon doping profile in an *n*-type DBR.

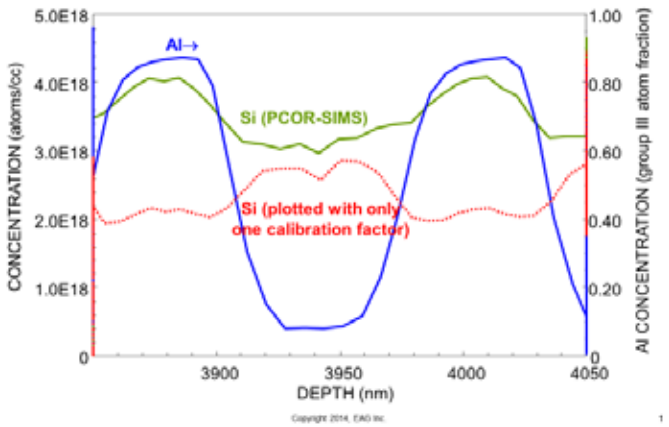

Figure 3. The PCOR-SIMS technique is capable of accurate measurements of the silicon concentration independent of the aluminum concentration.

PERFECTING THE VCSEL

Producing a very high performance VCSEL requires optimization of various aspects of the device, including: the aluminum composition and gradient between high and low refractive index mirror layers; the dopant profile between mirror layers; the composition of the aperture layer (assuming it is an oxide-confined VCSEL); the active layer impurity content; the aluminum grading on either side of the active layer; and, of course, the thicknesses of all of the layers within the structure.

An example of a PCOR-SIMS depth profile of a complete VCSEL structure is shown in Figure 2. This wafer uses a carbon-doped p-type AlGaAs DBR, a silicon-doped n-type DBR and an undoped, low- AlGaAs active layer with a multi-quantum well.

If the DBR is to provide good current injection, it must have a low electrical resistance. Realizing this in a manner that produces a good device is not trivial. Large energy band offsets between the low and high index semiconductor layers of the DBR can inhibit current flow, particularly for p-type DBRs – and the obvious solution of increasing the doping to trim resistance is not an option because this increases optical absorption.

A far better approach is to grade the AlGaAs composition at the interfaces, while varying the doping profiles at these points. In due course we will show how PCOR-SIMS is uniquely capable of measuring subtle alloy grading and interface doping profiles.

To obtain a high efficiency and low threshold current, the VCSEL must confine both the carriers and the transverse optical modes. Today, this is often realized in AlGaAs VCSELs through the selective oxidation of a very high Al-content AlGaAs layer, which is near the active layer (this creates so-called 'oxide-confined' VCSELs). One challenge with this design is to control the oxidation of these layers: to form the confining aperture correctly and reproducibly. The composition of the Al0.98 Ga0.02 As layer must be controlled to 1 percent. Later in this article, we will demonstrate how PCOR-SIMS can aid the wafer grower by measuring the composition of the AlGaAs layer with this level of precision and accuracy.

Obviously, another pre-requisite for the successful growth of a VCSEL epi wafer is to accurately control the thicknesses of the many layers that make up a working device. Nowhere is this more important than in the DBR, where the thicknesses must be correct to tailor the optical properties of the mirrors.

However, one must not neglect the importance of obtaining the correct thickness for the cladding and active layers, because this is needed to place the lasing mode optimally with respect to the boundaries of the 1λ-optical cavity. As we will soon see, when the growth engineers turn to PCOR-SIMS, they can correctly measure the composition of each layer, and as well as the correct layer thicknesses.

Understanding VCSELs: From Epitaxial Wafer Growth to Failure Analysis

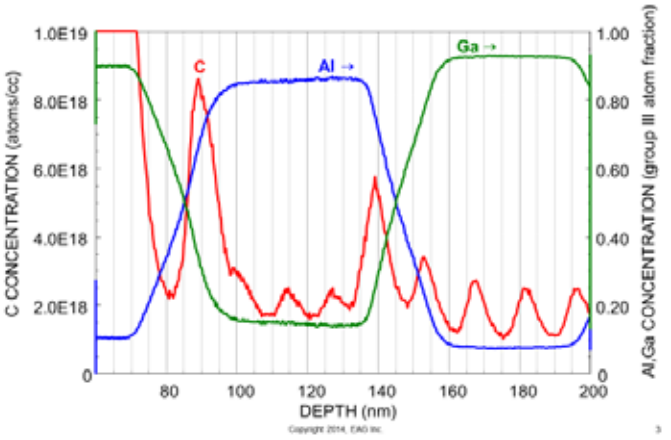

Figure 4. Accurate carbon concentration and depth placement in AlGaAs layers with a graded composition. Note that the low-level carbon dopant peaks may originate from a non-uniformity in doping, while the wafer was rotated during layer growth.

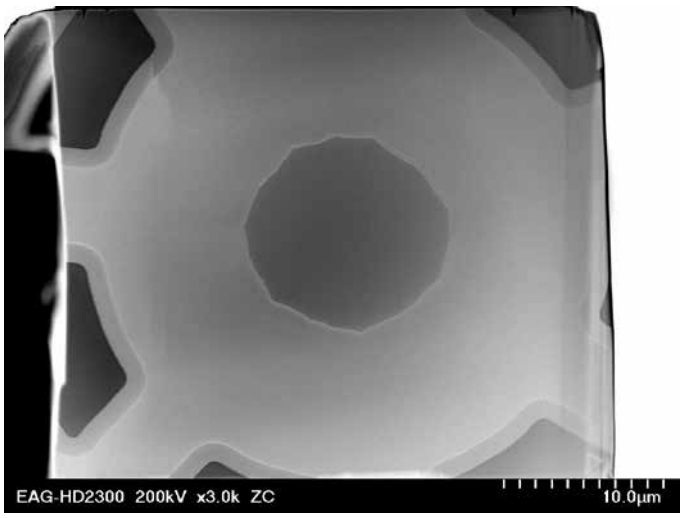

Figure 5. Plan view (PV) scanning transmission electron microscope (STEM) image of an entire VCSEL mesa. The oxidation of the aperture layer proceeds from the outer edge of the large ring toward the center. The darker, center portion of the image is the unoxidized region through which the current and light must travel.

SCRUTINIZING THE STRUCTURE

We have used our novel PCOR-SIMS technique to analyze a VCSEL structure with a carbon-doped p-type AlGaAs DBR, a silicon-doped n-type AlGaAs DBR and an un-doped, low-aluminum AlGaAs active layer containing a multi-quantum well. We will show how our technique can offer insights into the alloy composition profile, the DBR dopant profiles, and various details associated with the active layer.

As previously mentioned, grading the alloy composition between the low and high index layers can trim the resistance of the DBR. With our PCOR-SIMS technique, it is possible to home in on this part of the structure. Figure 4 is a higher depth-resolution profile of the top 200 nm of a p-DBR revealing the compositional grading.

The composition grading occurs because the aluminum and gallium are not simply 'switched on or off' but varied in a precisely controlled manner to optimize the optical and electrical properties of the interfaces. Measurements with PCOR-SIMS have determined the aluminum content correctly over the entire range of composition, from 8 percent to 83 percent aluminum. The accuracy of these measurements has been verified against Standard Reference Material 2841 ($Al_{0.1982\pm0.0014}Ga_{0.8018}As$) from the National Institute of Standards and Technology and a Rutherford Backscattering Spectrometry calibrated, multi-composition AlGaAs reference material.

Further reductions in the resistance of the p-type DBR are possible by doping the mirrors with carbon, which has a sensitivity that is significantly affected by the alloy composition. However, with PCOR-SIMS we can correct for these effects at every data point, because the aluminum composition is measured for every carbon data point. Such an approach uncovers a high-concentration carbon-doping spike which is near, but not exactly at, the interface between the low index layer with the higher aluminum content and the high index layer the lower aluminum content (see Figure 4).

We are confident that the placement of the carbon-doping spike is correct, because all the profiles were acquired in the same analysis. Note that the low-level carbon dopant peaks may originate from a non-uniformity in doping, while the wafer was rotated during layer growth.

To provide current and optical confinement, producers of VCSELs often introduce a high-aluminum-content AlGaAs layer which is oxidized from the outside inwards. Halting the process at an appropriate point leaves an unoxidized "aperture" through which current and light must pass. Figure 5 shows a low magnification, plan view scanning transmission electron microscope (PV STEM) image of such an oxidized aperture layer.

Obviously, to have a repeatable oxidation process, the rate of oxidation must not vary. This implies that there must be stringent compositional control and uniformity for the AlGaAs layer, because oxidation rates can vary by more than two orders of magnitude when aluminum content is increased from $Al_{0.82}Ga_{0.18}As$ to $Al_{1.0}Ga_{0}As$.

With PCOR-SIMS, the aluminum composition in high-aluminum-content AlGaAs layers, such as those used in forming aperture layers, can be determined with a high level of precision (see Figure 6). In these samples, the difference in aluminum content is only 1.8 percent of the of the Group III composition – or 0.9 percent of total atoms –but the spread in the measurement values of either

Understanding VCSELs: From Epitaxial Wafer Growth to Failure Analysis

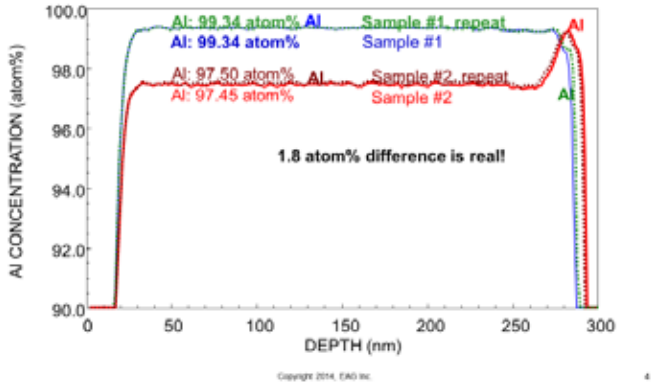

Figure 6. PCOS-SIMS showing composition differences of AlGaAs with high precision.

film is much less. This degree of measurement precision is crucial in perfecting these aperture layers.

Determination of the correct layer thickness with conventional SIMS is not easy, because changes in alloy composition alter the sputtering rate (AlGaAs sputters slower than GaAs). If no corrections are made, the plotted layer thickness for the DBR layers can be in error by 20 percent for an AlGaAs VCSEL (see Figure 7). With PCOR-SIMS this weakness is addressed with an empirically derived sputtering-rate function. This determines the instantaneous sputtering rate for each data point based on the measured aluminum content for that data point (or for indium content for InGaAs active layers). Armed with this approach, compensation corrections are made for variations in sputtering rate throughout the VCSEL.

PCOR-SIMS can also offer insights into the structure of the active region (see Figure 8). It can reveal the aluminum profile, which

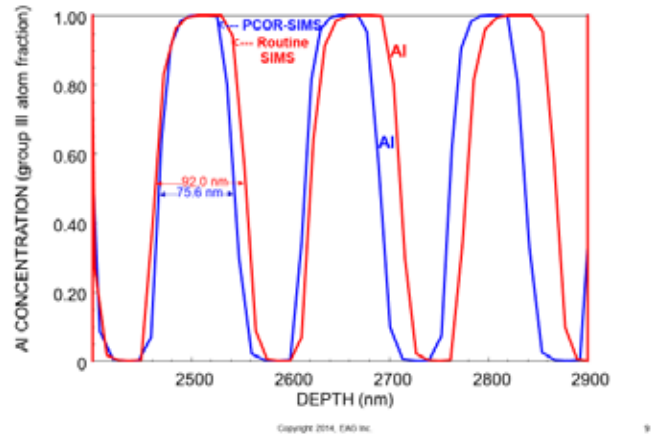

Figure 7. A depth profile of an AlGaAs DBR layer, showing the PCOR-SIMS layer-thickness correction, in comparison with regular SIMS calibration.

varies on both sides of the active layer. There is grading from the p-type aperture layer, and from the n-type DBR to the cladding layers, where it is followed by a steep drop in aluminum content, which is lower in the barrier layers immediately surrounding the AlGaAs active layer. A detailed picture of the active region is also helpful for assessing whether the lasing mode in the optical cavity is in the optimal position.

The profile of the active region in Figure 8 also details the carbon doping for the active region and the mirror pairs nearby. The doping

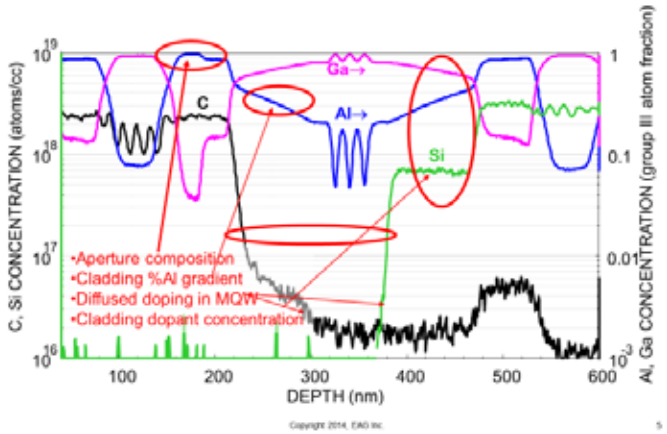

Figure 8. Depth profile of the active region detail: (a) aperture layer composition; (b) gradient in cladding layer aluminum content; (c) cladding layer dopant concentration; (d) diffused doping in a multi-quantum well. Note the rising carbon profile in the *n*-type DBR. (Note that nearly all the *p*-DBR has been removed by chemical etching.)

level in the MQW should be as low as possible. By measuring carbon and silicon concentrations accurately in the ***n***-type DBR with PCOR-SIMS, it is also possible to determine the amount of ***p***-type counter-doping that the inadvertent carbon contamination causes in the *n*-type layers.

You will notice, however, that in Figure 8, the MQW layers in the active region are not fully resolved because they are so thin, and SIMS has the unavoidable artifact of atomic mixing of the layers by the primary ion beam used for sputtering. Fortunately, EAG Laboratories can bring multiple tools to bare on a problem. Figure 9 shows a cross-section STEM (XS STEM) image of a MQW region of a VCSEL. Not only does STEM's sub-Angstrom resolution fully resolve each layer, but the actual layer thicknesses can be measured with sub-nanometer precision.

Understanding VCSELs: From Epitaxial Wafer Growth to Failure Analysis

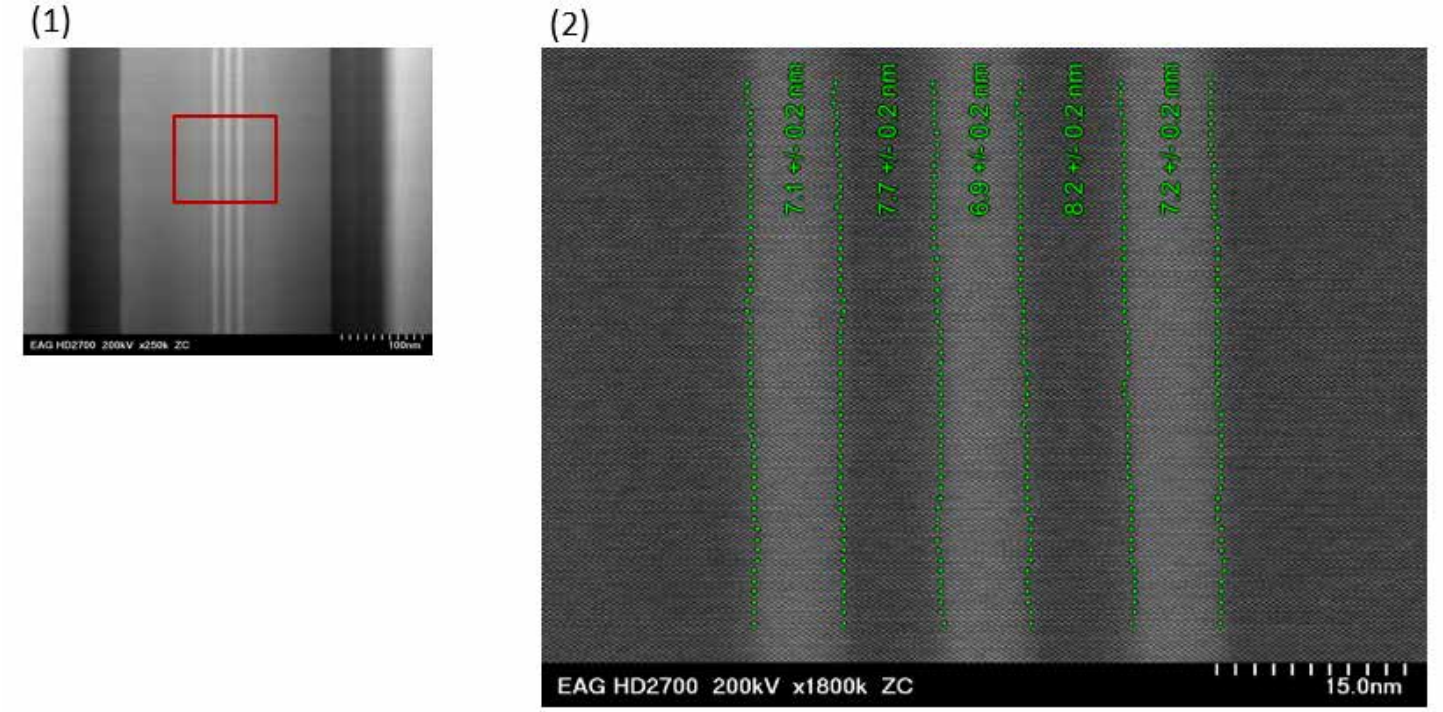

Figure 9. (1) Lower magnification STEM image of the multi quantum well region, (2) Higher magnification image shows the average layer thicknesses as well as the standard deviation of each thickness measurement. Precise and automated thickness measurements provide more quantitative results than measuring by eye.

In addition, the incomplete resolution of the multi quantum well layers in figure 8 also results in inaccurate aluminum and gallium concentrations in those layers. However, we again use cross section STEM imaging, but this time with energy dispersive X-ray spectrometry (EDS), to obtain more accurate Al and Ga concentrations in these fully resolved, thin active-region layers as shown in Figure 10.

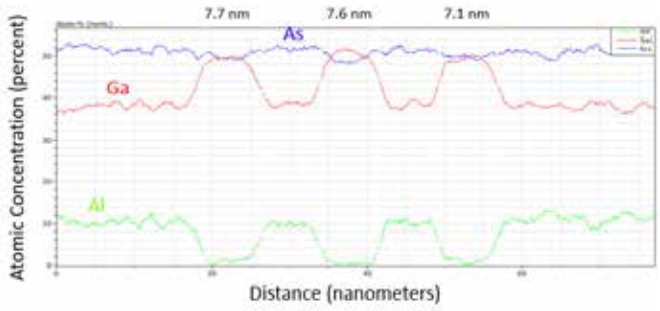

Figure 10. STEM/EDS line scan across the MQW region of a VCSEL showing not only the layer thicknesses but also the concentrations of Al and Ga in the active region.

Figure 11 shows how we can utilize Spherical **A**berration **C**orrected **STEM** (AC-STEM) combined with EDS mapping to further interrogate the VCSEL structure and composition with extremely high spatial resolutions. This high-resolution analysis capability is important in certain cases, where nano-scale ordering at interfaces is to be investigated which otherwise are unobservable by regular STEM, or SIMS because they are averaged out by the typical analytical sampling.

This approach requires very thin, low-damage lamellae, prepared via FIB. These highly localized compositional inhomogeneities create nm scale roughening of the interfaces throughout the epi stack. In this example this is especially true for the surface side of the AlGaAs aperture layer as well as the AlGaAs/GaAs p-DBR interfaces. Since the oxidation process is very sensitive to Al and Ga compositions, the nanoscale ordering at these interfaces complicates the resulting aperture oxide morphology, composition, and chemistry, as well as the p-DBR layers at the edge of the mesa. These extremely subtle structural differences can ultimately drive the underlying device reliability and performance issues once the devices are put into service.

Understanding VCSELs: From Epitaxial Wafer Growth to Failure Analysis

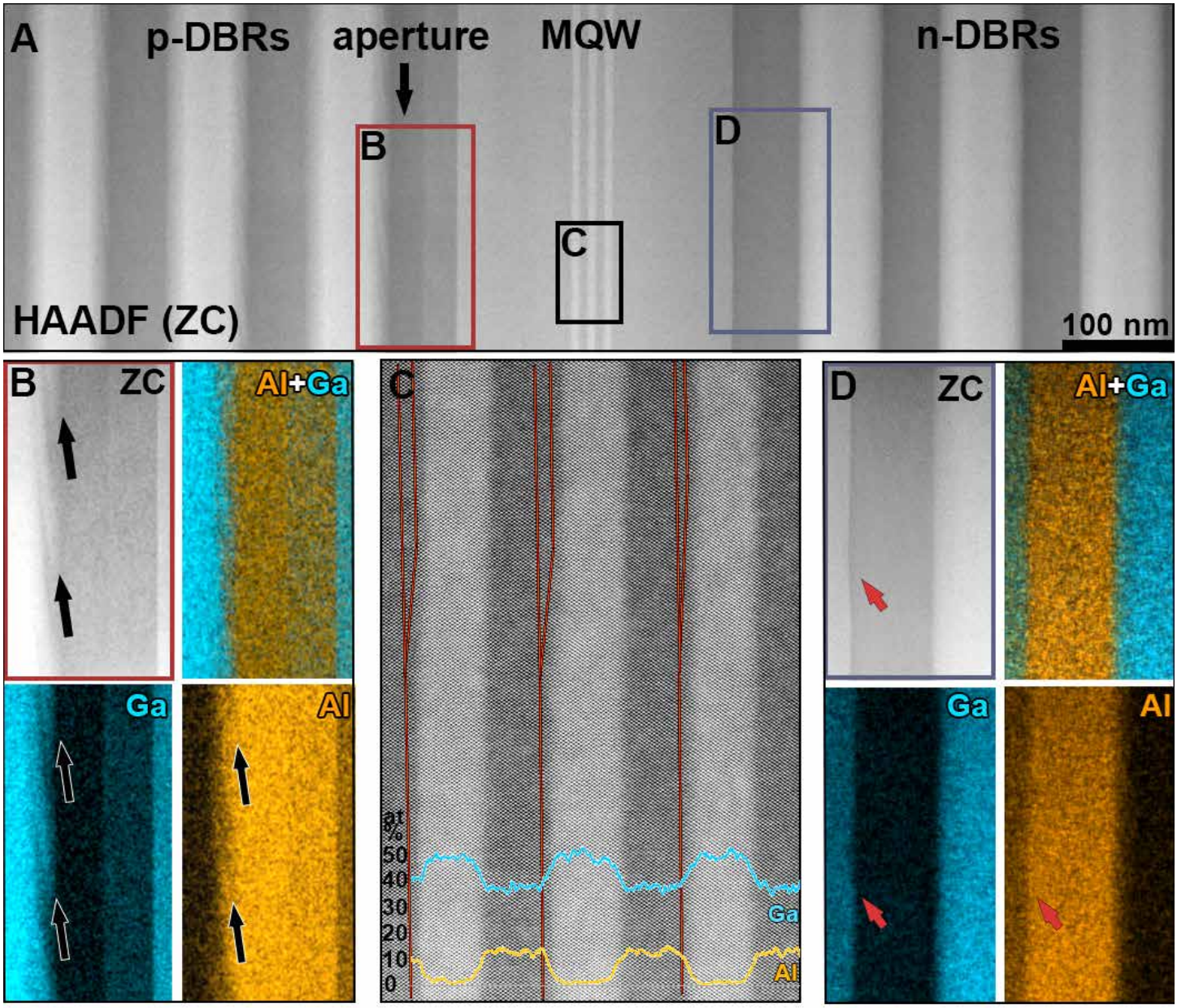

Figure 11. AC-STEM imaging and EDS mapping of an unoxidized VCSEL epi sample around MQW region. An overview of the structure is seen in (A). Z-Contrast (ZC) imaging using High-Angle Annular Dark Field (HAADF) is utilized to create sub-Angstrom spatial resolution images where the intensity roughly scales to the Avg. atomic number (Z) at each pixel. The brighter the intensity, the higher the avg. Z, allowing for the observation of small, ~10nm, composition fluctuations occurring in the AlGaAs layers. Inset (B) shows these fluctuations (denoted by black arrows) occurring on the surface side of the aperture layer in both ZC imaging as well as EDS mapping, showing highly ordered compositional gradients within the transition from the aperture layer to the GaAs p-DBR layer. Inset (C) shows the MQW region and that there are significant changes in the MQW layer thicknesses that occur periodically (red lines) resulting from steps that form during growth. Inset (D) shows that there is also evidence of steps occurring n-DBR.

Understanding VCSELs: From Epitaxial Wafer Growth to Failure Analysis

FAILURE ANALYSIS OF VCSELS

SIMS in Failure Analysis

Another strength of PCOR-SIMS is its ability to profile unwanted contamination species. The most ubiquitous of these is oxygen. The Al-containing precursors (such as trimethylaluminum) used in the metal organic chemical vapor deposition (MOCVD) growth of VCSELs are easily contaminated with OH or O which can seriously degrade the non-radiative carrier lifetime in optoelectronic devices with more than a few percent aluminum as VCSELs have. Inadvertently introduced O can also create scattering centers which decrease mobility. Thus, it is imperative that oxygen contamination in the active layer of the device be kept as low as possible. Oxygen contamination spikes can also be introduced at the growth transition between the low index and the higher index layers of a p-type DBR as shown in Figure 12).

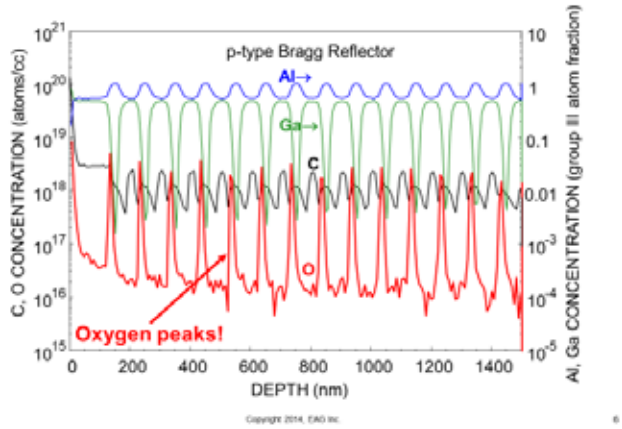

Figure 12. PCOS-SIMS can reveal oxygen contamination spike at DBR interfaces.

Knowing the exact location of oxygen spikes in the growth sequence is often helpful when trying to isolate and eliminate the source of contamination.

Occasionally, VCSELs contain sulfur impurities as shown in Figure 13. Like oxygen, sulfur is also believed to affect the non-radiative carrier lifetime performance. It is believed that the sulfur originates from the substrate, perhaps from a surface-cleaning step. During the growth of the *n*-DBR region, the sulfur segregates to the growing surface and is not incorporated into the *n*-DBR, But as soon as the aluminum starts to rise in the p-cladding layer, with an accompanying change is growth temperature for the p-DBR the sulfur abruptly stop most of its diffusion to the growing surface and becomes incorporated at the start of the p-cladding layer.

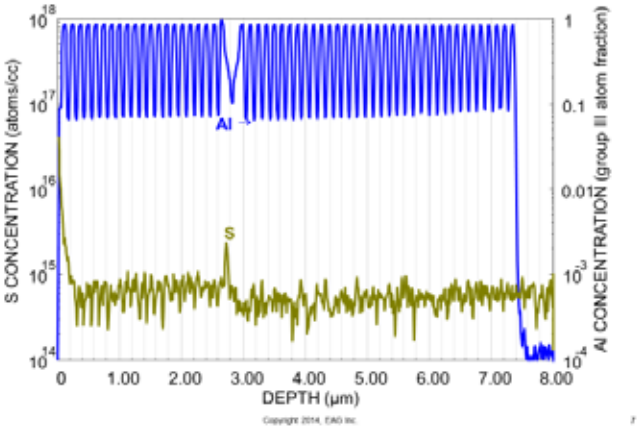

Figure 13. Sulfur impurities, which may degrade VCSEL performance, can be detected in many layers of this VCSEL structure.

This is shown in greater detail in Figure 14.

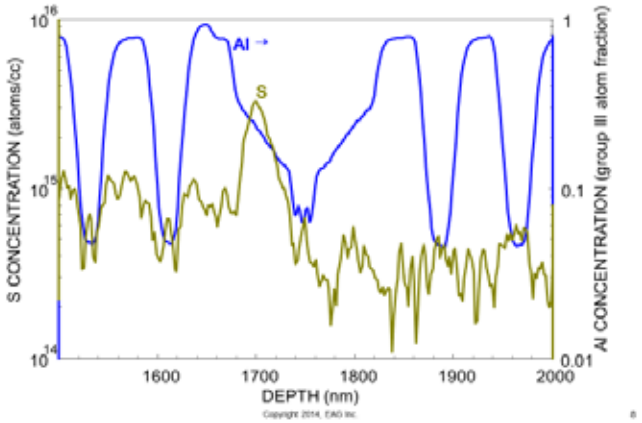

Figure 14. A peaking sulfur impurity is detected in upper AlGaAs p-cladding layer. Higher sulfur levels are often found in the p-DBR relative to the n-DBR.

STEM in Failure Analysis

The primary failure modes for most VCSELs include the formation of crystalline defects within the complex epitaxial structure which eventually migrate under operation into the active layers, killing the device. These failure modes often have characteristic defect morphologies and electrical responses that are directly related to the way in which they are failing. To positively categorize the failure as resulting from ESD, corrosion, overstress, etc., it

Understanding VCSELs: From Epitaxial Wafer Growth to Failure Analysis

is important to understand both the extent and overall defect structure within the VCSEL as well as the L-I-V characteristics of these failing devices. (A useful resource for understanding the range of typical ESD failure modes and how to identify them can be found here: https://www.finisar.com/sites/default/files/downloads/reliability_data_an_atlas_of_esd_failure_signatures_in_vertical_cavity_surface_emitting_lasers.pdf)

The electrical and optical data is typically fairly straight forward to acquire, but since the analytical area of VCSELs are on the order of 10s-100s of um^2, there are several challenges to overcome when trying to capture the entire extent of the defect network as well as pinpointing the specific defect location that initiated it. Optical characterization techniques, such as Electroluminescence Imaging (EL), can help us understand the uniformity of emission as well as assess where damage is located (active layers, mirrors, or both), but the spatial resolution is limited making it very difficult to distinguish specific defects. Additionally, imaging of the devices from the emission side limits the optical inspection to the aperture region as the surrounding portions of the mesa are typically covered by the p-contact metallization. To overcome this, optical inspections can often be performed from the backside of the device through the substrate after careful mechanical preparation, but this incurs additional loss risk and still does not achieve resolutions required to track individual dislocations. It is important to have both an imaging technique that can observe these defects as well as a sample preparation technique that mitigates the risk of loss for these one-of-a-kind samples.

It turns out that scanning transmission electron microscopy (STEM) combined with Focused Ion Beam (FIB) sample preparation is an ideal technique for root cause failure analysis (FA) of VCSELs. STEM imaging combined with EDS can provide both the crystallographic as well as compositional information about a sample across a wide range of length scales in both Planview (PV) and Cross-section (XS). Sample preparation by FIB removes material from the regions adjacent to the target location and the remaining sample is lifted out (LO) in-situ utilizing a micromanipulator and welded on to a standard Cu TEM support grid. Figure 15 shows a FIB-cut Cross-section (XS) lamella welded to the lift out (LO) needle, being lifted out, ready to be welded a TEM grid.

This in-situ LO technique always maintains physical control of the sample. The lamella is first securely attached to the LO needle and then welded to a TEM support grid, which can then be handled by tweezers and moved between instruments safely. Samples are only final thinned to electron transparency once they are safely welded to the grid. Individual lamella can be further processed in the FIB if deemed necessary after STEM inspection.

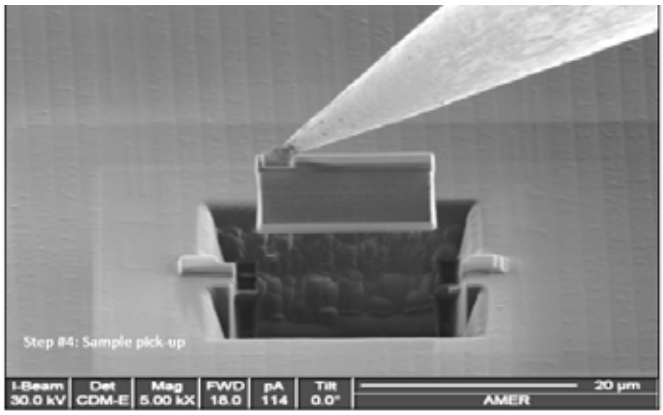

Figure 15 shows a FIB-cut thin sample being lifted out and ready to be placed on a TEM grid.

This includes thinning, surface damage removal, XS from PV, etc. (For an overview of TEM/STEM at EAG, please see: https://www.eag.com/techniques/imaging/tem-stem/)

Specifically, for VCSEL STEM FA, a FIB prepared PV lamella that is 40um x 40xm and ~ 1um thick is typically utilized. Figure 16 shows an example of this preparation and the resulting STEM data. The lamella covers the extent of the entire mesa (save a small amount of one edge) and contains the active MQW layers along with the oxidized, high-aluminum-content AlGaAs aperture layer and several DBR repeats on either side within the 1 um thickness. This data allows for the determination of overall failure mode character as well as providing specific location(s) for subsequent FIB XS extraction to examine specific suspect out of plane (OOP) defects as they evolve through the epitaxy. It is often the OOP dislocations that hold the key to determining the root cause within a certain failure mode. PV-STEM imaging and in-situ marking of the PV provides nm precision for the extraction of additional XS(s) and is nearly 100% successful at targeting the suspected defect.

The aperture layer is well known the weakest point in VCSEL devices and there are several major issues EAG has been working on to understand point of failure. Fast-growing dark line defect (DLD) failures are responsible for nearly all observed failures in VCSELs, so it is important to know how they initiate. In one way or another, nearly all the DLDs trace their origin to mechanical stress or damage such as a crack in the die or over oxidation of various layers. It could be handling-related, a grown-in defect, or from electrostatic discharge (ESD). Regardless, the DLD grows toward the emitting area as the device is operated, eventually killing the device. An example of a typical DLD network starting from the aperture oxide is seen in Figure 16.

Understanding VCSELs: From Epitaxial Wafer Growth to Failure Analysis

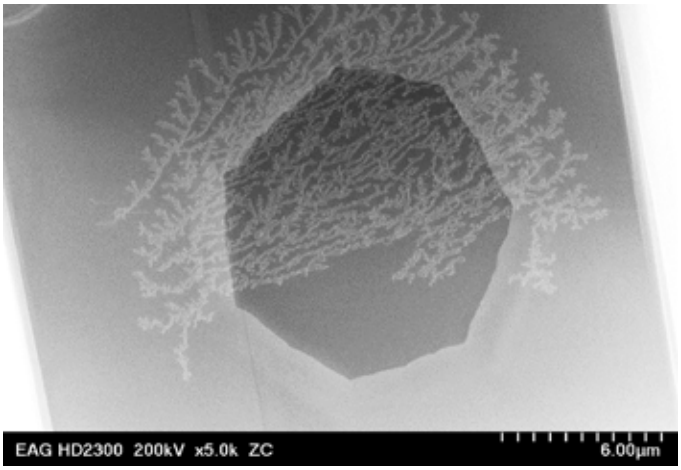

Figure 16. Higher magnification view of aperture region of a failed VCSEL showing DLD network.

In Figure 17, we show how we can utilize the STEM PV data to create a targeted XS (between yellow lines in (2)) isolating the OOP dislocations responsible for creation of the DLD in the MQW. Now viewed in XS, it is clear the DLDs began in the aperture layer at point (a) then propagated down to the MQW layers where the DLD grew extensively toward and past the aperture edge. Once past the aperture edge, the defects would degrade the carrier lifetime to the point where the device failed. However, one can also see that at point (b), the DLD also penetrated the n-cladding layer and migrated into the n-DBR where it propagated laterally before penetration further into the n-DBR at point c. While it can take thousands of hours for OOP dislocations to migrate from outside the device to the mesa region, once in the active layers, the DLD travels faster and faster as it gets closer to the emitting area, and the power driving the DLD growth increases. Once it gets close to the emitting area, it will go from having no effect to causing device failure in a matter of minutes to seconds.

In some situations, it may not be as clear whether the origin of the DLD is from the aperture layer or from some other source outside the extent of the PV lamella. The DLD network can become very complicated, or there can be many OOP dislocations, making it difficult to discern which OOP dislocation is "the one". It is then important to try to recreate certain confounding failures under similar high stress conditions in the lab and to ideally catch the failure as early as possible using a combination of EL and STEM. An example of this type of study is shown in Figure 18 and Figure 19. Since there are detectable changes in the light output due to the presence of DLD, thresholds can be set such that the defects are caught much earlier, before they have a chance to grow and consume a larger majority of the active region. This provides the needed clarity for identifying the source of the DLD using STEM.

STEM imaging can then be used to prove that the decrease in light output is due to damage from DLDs as well as their origin at the edge of the aperture. In Figure 19, (1) shows a low magnification PV-STEM image of the aperture in the aged device. One can see evidence of DLDs at the same location as the dark area in the

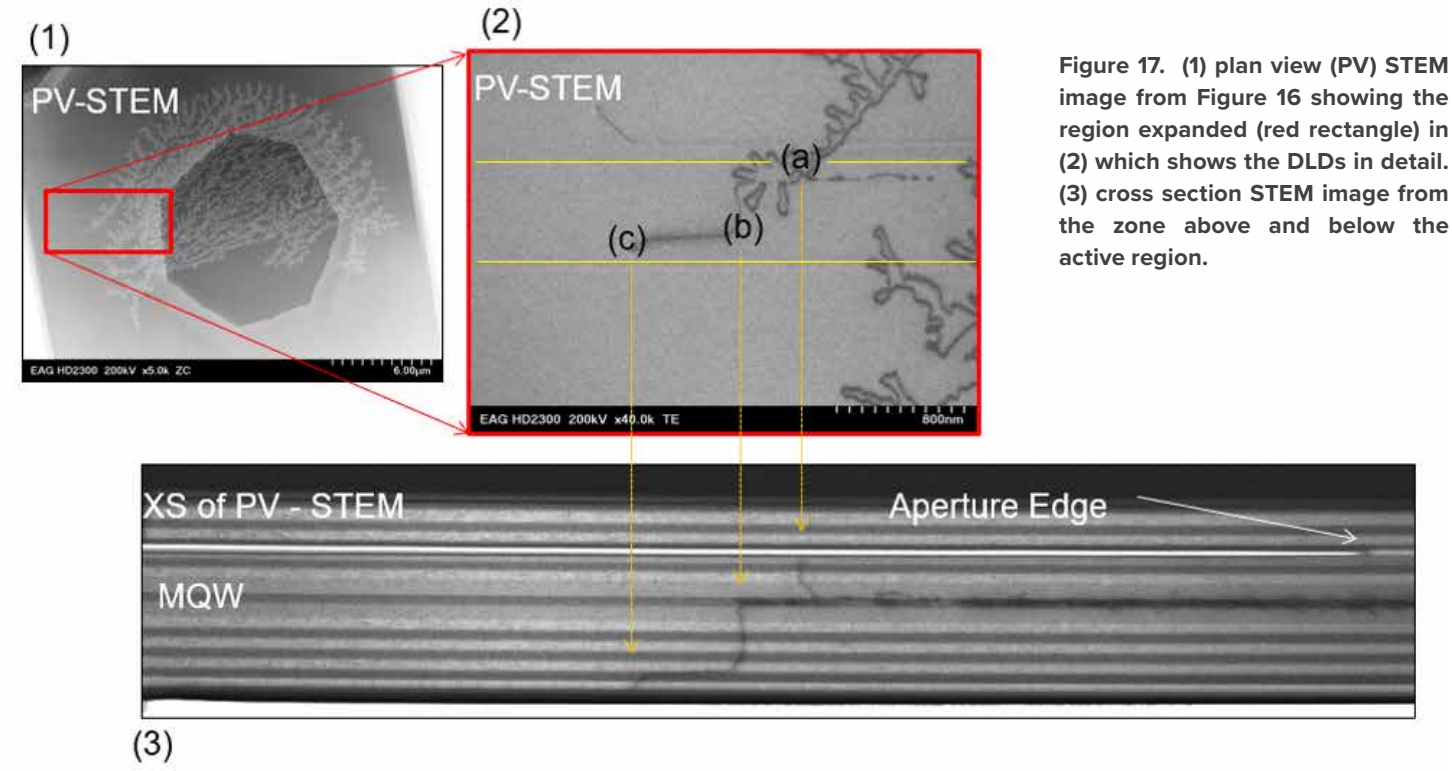

Figure 17. (1) plan view (PV) STEM image from Figure 16 showing the region expanded (red rectangle) in (2) which shows the DLDs in detail. (3) cross section STEM image from the zone above and below the active region.

Understanding VCSELs: From Epitaxial Wafer Growth to Failure Analysis

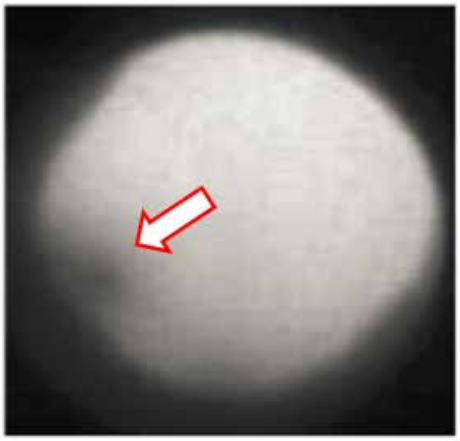

Figure 18. Electroluminescence image of aperture of a VCSEL showing early stages of effects of DLD damage to optical output of the device. This VCSEL was subjected to accelerated aging. It suffered a 26% decrease in output after aging at 70C 85%RH for 49 days @ 1mA followed by an additional 9 days @ 6mA. (See: *Corrosion-Based Failure of Oxide-Aperture VCSELs*, Robert W. Herrick, et. al., IEEE JOURNAL OF QUANTUM ELECTRONICS, VOL. 49, NO. 12, DECEMBER 2013)

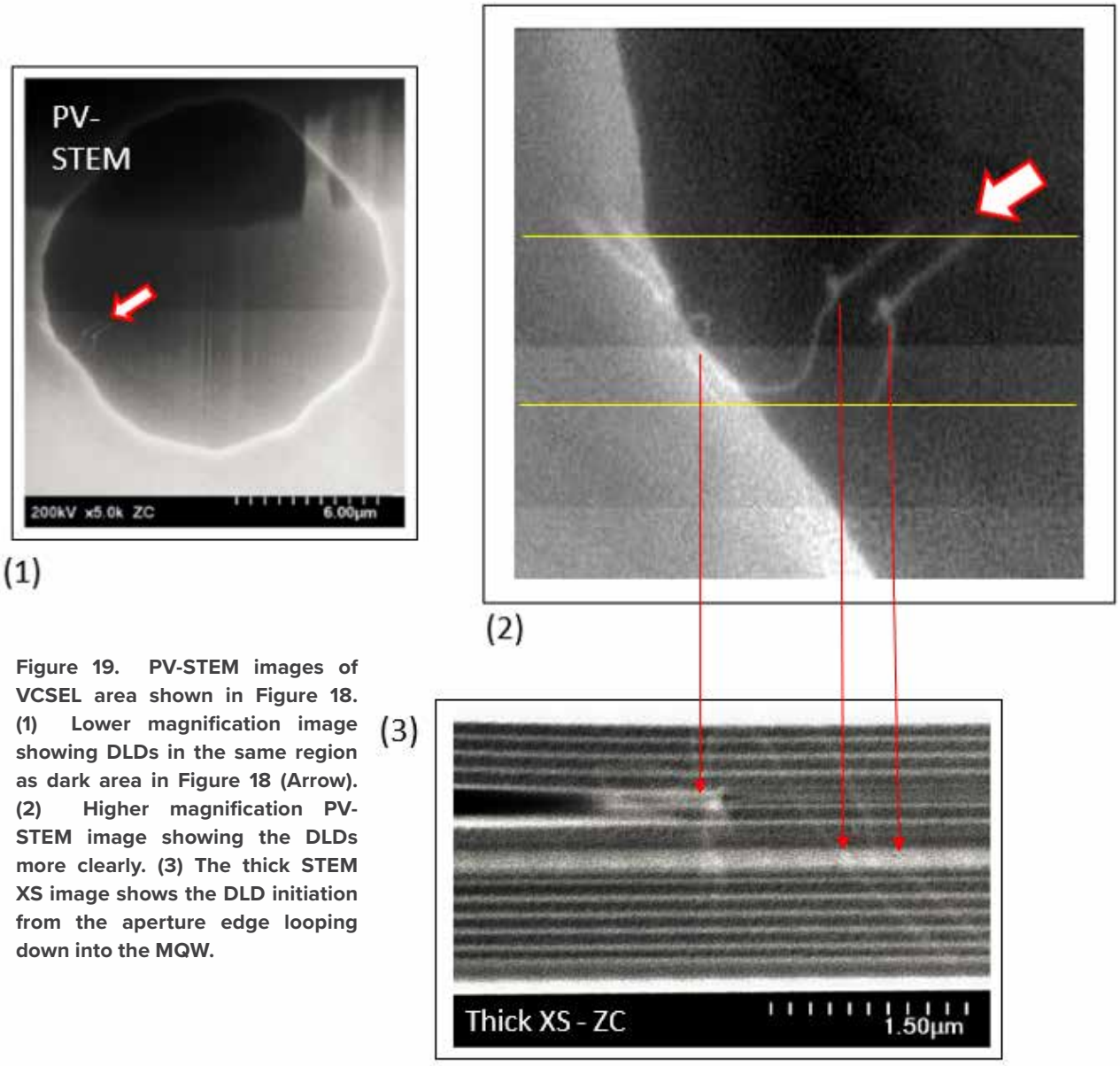

Figure 19. PV-STEM images of VCSEL area shown in Figure 18. (1) Lower magnification image showing DLDs in the same region as dark area in Figure 18 (Arrow). (2) Higher magnification PV-STEM image showing the DLDs more clearly. (3) The thick STEM XS image shows the DLD initiation from the aperture edge looping down into the MQW.

Understanding VCSELs: From Epitaxial Wafer Growth to Failure Analysis

EL image of Figure 18. The DLDs are clearly seen in the higher magnification image in panel (2) of Figure 19. One can see that in this failure the DLDs were initiated at the edge of the oxide aperture which we noted above is a prime place for weakness in an oxide confined VCSEL. Panel 3 of Figure 19 (STEM XS image of the DLD's) shows this. This allows for the early detection of possible device failures which can be important in increasing large scale reliability.

CONCLUSION

Our development of advanced techniques for materials analysis has allowed EAG Laboratories to provide comprehensive process development and failure analysis of vertical cavity surface emitting lasers. Our proprietary PCOR-SIMS capabilities have opened up this technique so that it is no longer limited to impurity and dopant analyses of semiconductor materials. This effort has enabled PCOR-SIMS to be a valuable tool for the growers of VCSELs. It can used for various important tasks, including accurate measuring of doping levels in graded layers and delivering precise values for the aluminum composition in AlGaAs aperture layers. It has also proved valuable in failure analysis of these devices when the failures are caused by inadvertent contamination. STEM and AC-STEM, have proven invaluable in EAG's efforts to understand device failure mechanisms in VCSELs providing the important mapping of DLD networks and epi characterization. Our advanced FIB sample preparation methods, developed over the last 15 years, are the key to our unmatched high data quality and analysis flexibility. Many of the same methods covered here are applicable to analyzing similar failure mechanisms in other optical devices such as ridge lasers, photodiodes, LEDS, etc.

ACKNOWLEDGEMENTS

Wei Ou, Jeff Serfass, Houston Dycus and Ozgur Celik contributed to this article.

FURTHER READING

Ueda O., Herrick R.W. (2013) Failure Analysis of Semiconductor Optical Devices. In: Ueda O., Pearton S. (eds) Materials and Reliability Handbook for Semiconductor Optical and Electron Devices. Springer, New York, NY

Reiner et al. IEEE Photon. Technol. Lett. 7 730 (1995)

https://www-s.nist.gov/srmors/view_detail.cfm?srm=2841

Sadao Adachi J. Appl. Phys. 58 R1 (1985)

K. D. Choquette et al., Electron. Lett. 30 2043 (1994))

SIMS Depth Profiling of SiGe Structures using Both Oxygen and Cesium Primary Ion Bombardment: a Comparison International conference; 12th, Secondary ion mass spectroscopy; 1999; Brussels